SUPPLEMENTAL FIGURES & METHODS.

Structural models of CapD. The crystallographic coordinates of CapD from *B. anthracis* with PDB code 3G9K contain two molecules within an asymmetric unit and have resolution of 1.8 Å (*25*). The two molecules differ significantly in conformation. The active site of one of the molecules contains a bound ligand and corresponds to a closed conformation, whereas the other molecule has a vacant active site and is in the open conformation. In addition, the structure in the closed conformation exhibits a conformational change of the side chain of Arg-520 in response to ligand binding. The first 28 residues of the protein are believed to contain a signaling peptide and are removed from the structure. Furthermore, some of the coordinates of the resulting two protein chains are missing due to disorder. The long (L) and short (S) chains of the molecules that are visible to X-ray span residues 46 to 337 and 352 to 528, respectively. The long chain has two internal gaps (between 118 and 125 and between 315 and 323) and is missing N-terminal residues through 46 and C-terminal residues starting from 338. The short chain has only an internal gap between residues 391 and 403.

The missing residues were modeled using the NEST program (*52*). In performing the modeling, we input both L and S chains simultaneously and built the loop between residues 338 and 352 in addition to the other missing loops. As this procedure attempts to refine the conformations of all the side chains present in the PDB according to its rotamer library, we combined the generated models with the PDB coordinates. This procedure preserves side chain conformations as much as possible as well as all of the structural water molecules from the PDB. In order to make integration of the model and PDB coordinates as smooth as possible, we identified regions of the closest RMSD distance near the boundaries of our final model. Based on that analysis we retained the original PDB coordinates for the following residues: 50 to 116, 126 to 313, 324 to 334, 352 to 390, and finally, 404 to 528.

To model the acylated CapD we used the modeled complex structures of CapD with PDGA-mimic models as starting coordinates. Subsequently, Thr-352 and capped γ-D-Glu were covalently linked. Where necessary, we derived new parameters using a compatible GAFF force field. In the final models, we capped the L chain (residues 46 to 337) with acetyl and N-methyl groups at the N- and C-terminus, respectively. The terminal residues 352 and 528 of the S chain were not capped. Upon inspection, the following protonation states have been assigned (using standard Amber notation): HIE L 55, HID L 89, HIE L 126, HIP L 140, HIP L 291, HIE S 354, HIP S 446. Finally, the models, including the protein coordinates derived as discussed along with their respective structural water molecules, were

solvated using tLEAP module of Amber Tools (*42*). Solvating the system produced a cubic box of water molecules with a minimum solvation shell around the protein of 10 Å. The energy and forces of the solvated system were generated from the Amber99SB force field (*42*).

Supplemental Scheme S1. Proposed mechanism for the *B. anthracis* CapD gamma glutamyl transpeptidase. The mechanism is based upon one proposed by Boanca et al. (*21*). We have included the Arg-432 and Arg-520 residues in the mechanism. Arg-520 acts as an electrostatic catalyst and is important in acceptor binding. Arg-432 is shown near the side-chain of the acceptor substrate. The roles of these residues were supported by our site-directed mutagenesis studies.

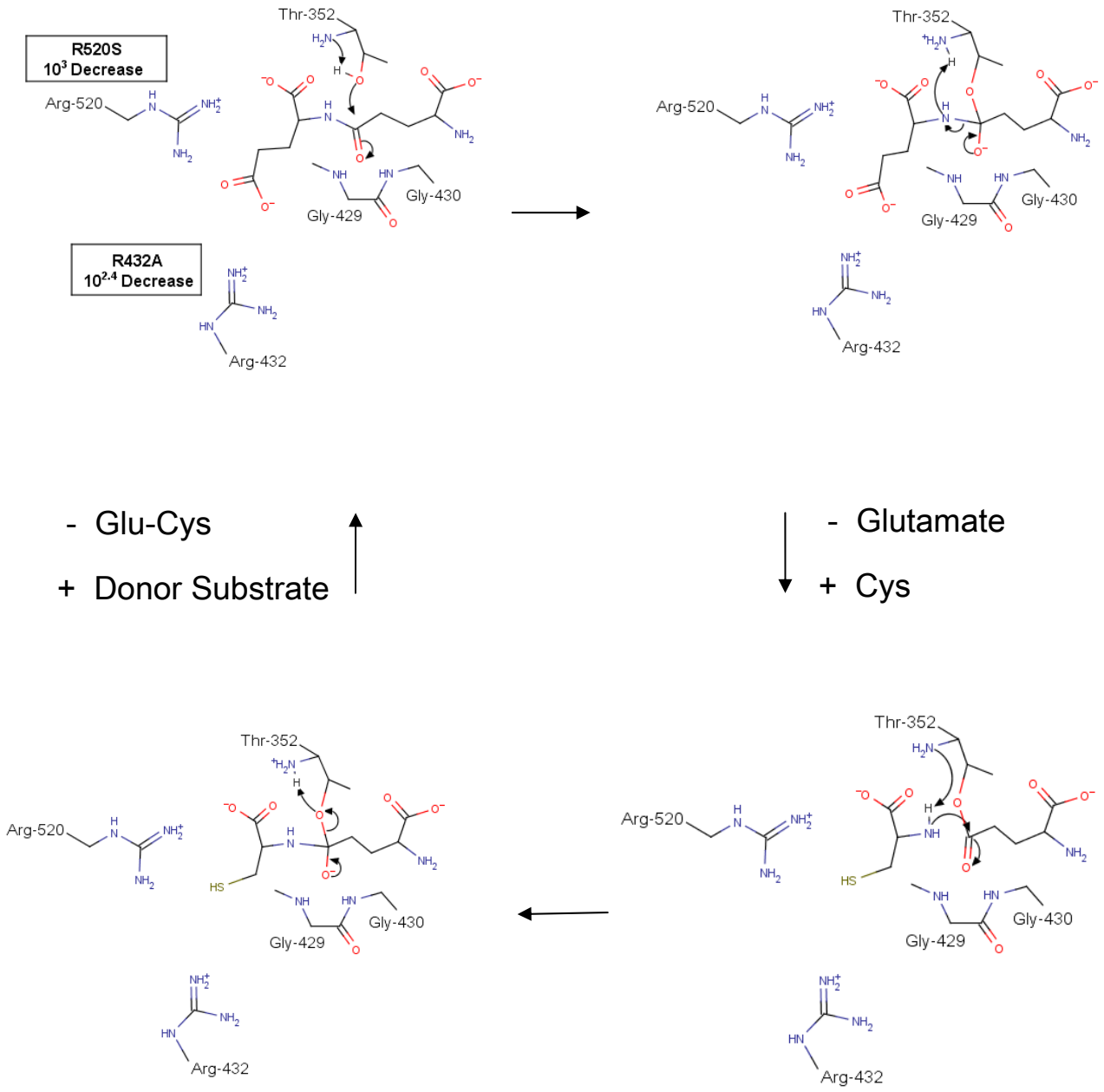

Supplemental Figure S1. The *B. anthracis* capsule degradation assay was described in the methods. Capsular material was purified from the Ames strain of *B. anthracis*. CapD was found to hydrolyze capsule more effectively in the presence of cell culture media. The components of the media were tested separately to determine which amino acids, metal ions, or nucleotides affected activity. Some amino acids in the media were found to enhance the activity of CapD (transpeptidation). The steady state kinetic parameters were determined for all 20 amino acids to determine the K_{ma} for each amino acid (**Table 1**).

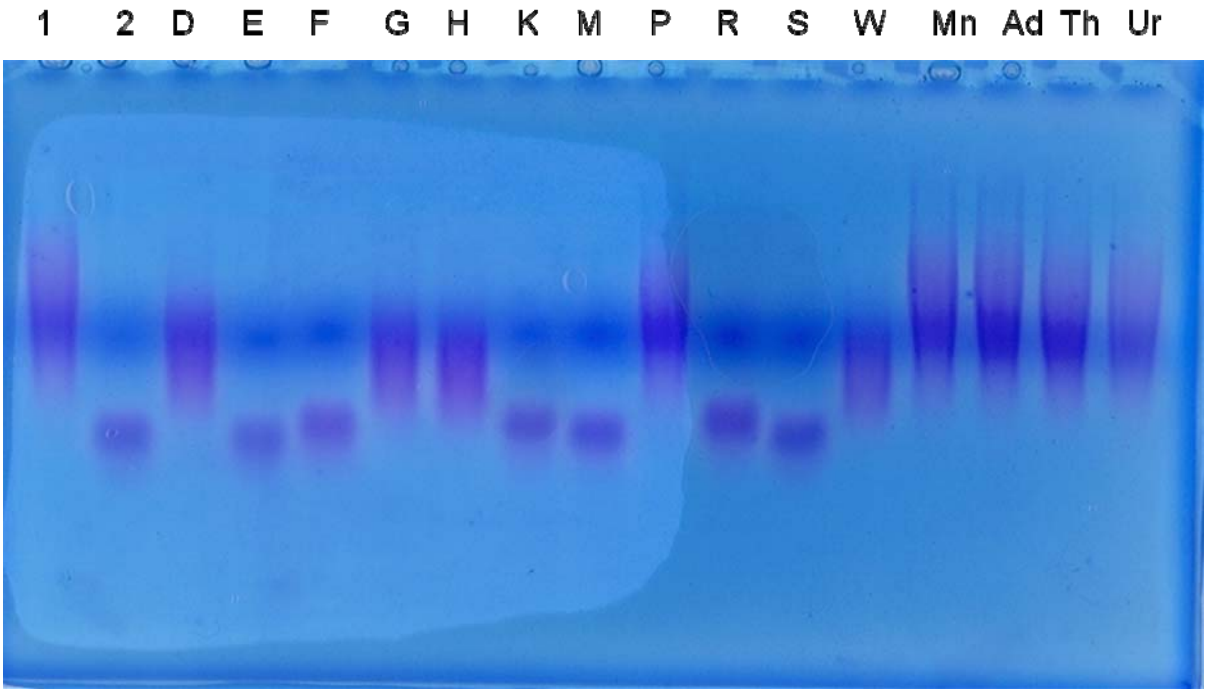

1 100 mM Tris pH 8.0

2 100 mM Tris + all amino acids

All samples contain 100 mM Tris pH 8.0, the indicated amino acid or additive, capsule and CapD (25 ug/ml). Reactions were incubated at 37 °C for 30 min

Abbreviations: Mn – Manganese chloride; Ad – adenine; Th – Thiamine; Ur - uracil

Supplemental Figure S2. Double reciprocal plot for CapD-MBP with varying concentrations of the L-serine acceptor substrate and FRET donor substrate. The data were globally fitted to yield a K_{ms} (FRET-substrate) = 13 ± 1 μM and a K_{ma} (L-serine) = 1300 ± 100 μM. The parallel lines observed in the double reciprocal plot are consistent with a Ping-Pong Bi Bi mechanism.

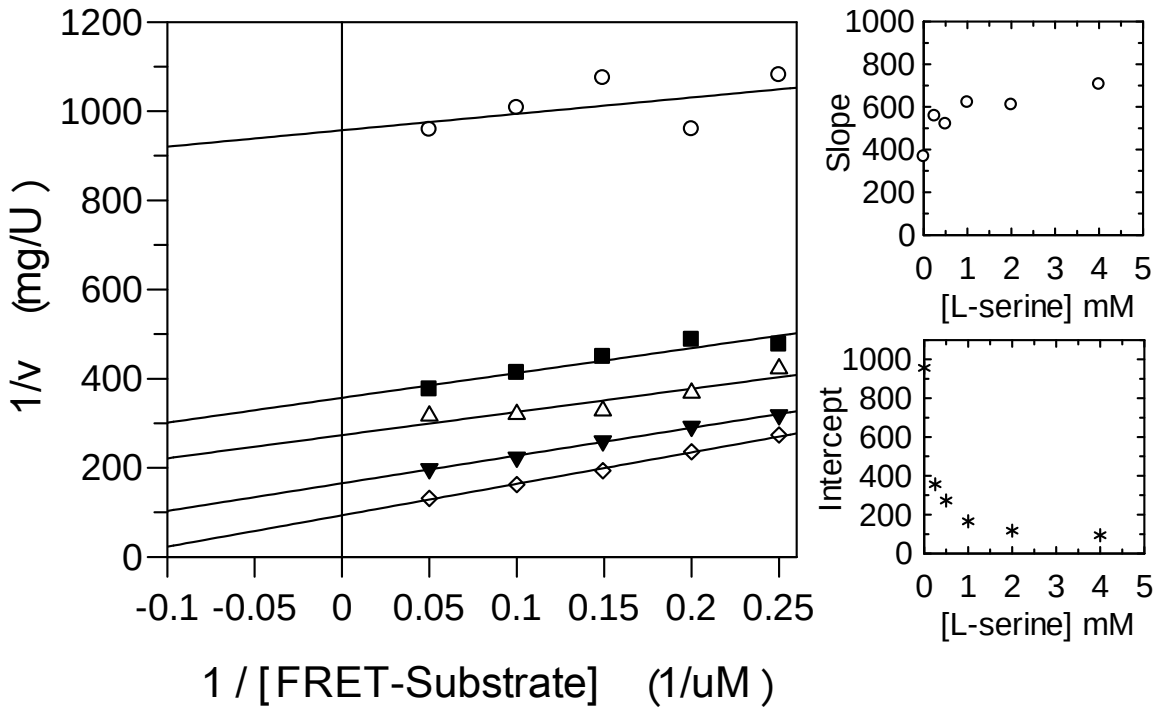

Figure S3. A model of γ-D-Glu-L-Cys in complex with CapD.

A model of the complex was derived using the Autodock Vina program. Carbon atoms of the CapD residues are shown in magenta, whereas those of the ligand are shown in green. Only polar hydrogen atoms of the protein are shown. Important residues for protein-ligand interactions are shown as sticks. Hydrogen atoms of the ligand are omitted for clarity. Pairs of atoms involved in hydrogen bonding are connected with dashed blue lines. The corresponding distances are shown in Å. Note the NH···S hydrogen bonding between the Cys and Arg-520 and Arg-432.

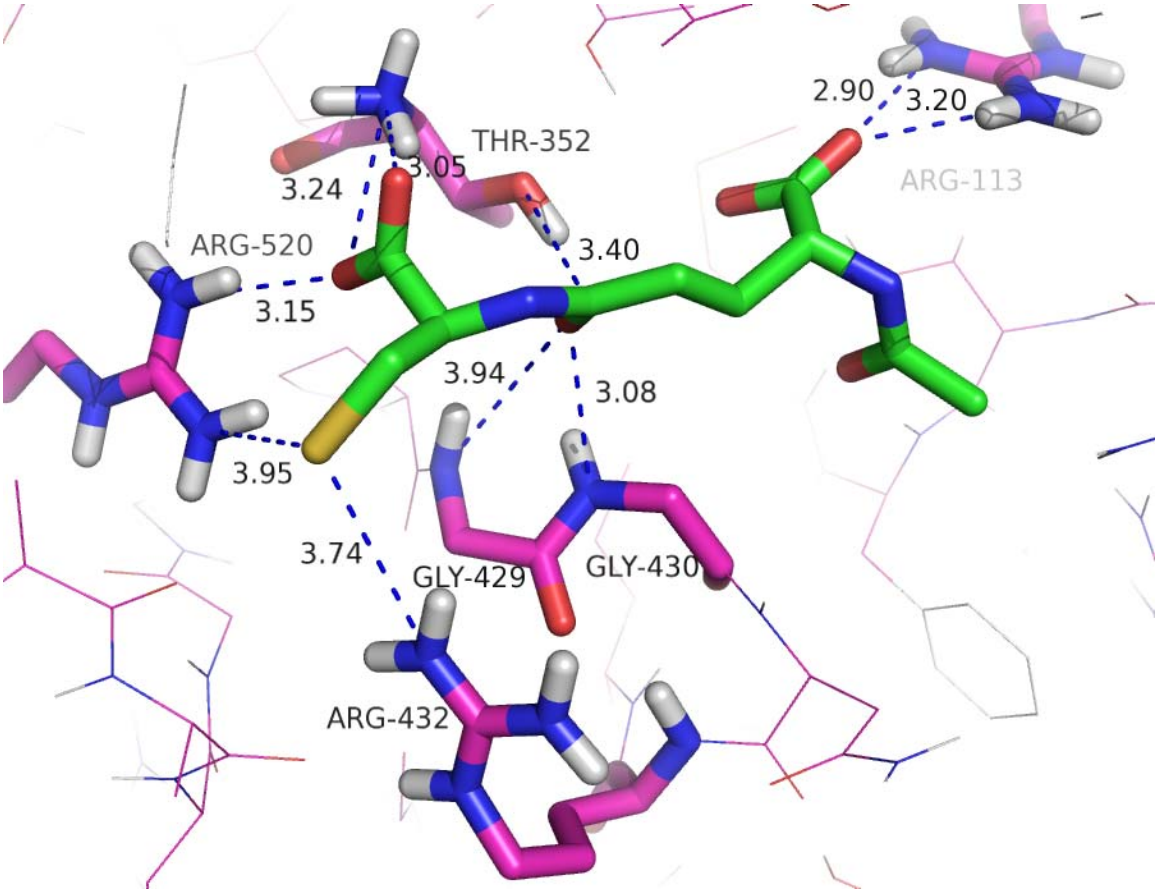

Figure S4. A model of the final γ-D-Glu-LMet in complex with CapD.

A model of the complex derived using the Autodock Vina program. Carbon atoms of the CapD residues are shown in magenta, whereas those of the ligand are shown in green. Only polar hydrogen atoms of the protein are shown. Important residues for protein-ligand interactions are shown as sticks. Hydrogen atoms of the ligand are omitted for clarity. Pairs of atoms involved in hydrogen bonding are connected with dashed blue lines. The corresponding distances are shown in Å. Note the NH···S hydrogen bonding between the Met sulfur and arginines.

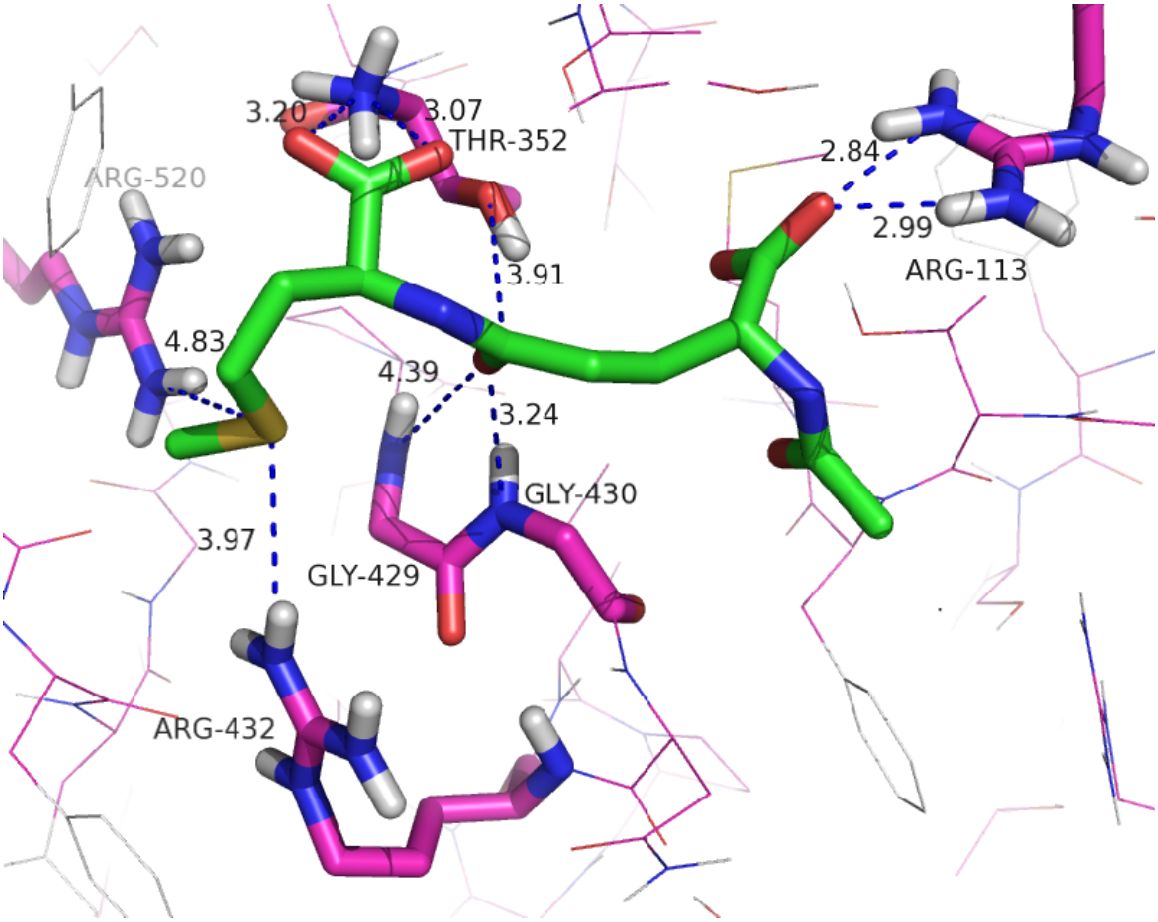

Supplemental Figure S5. Structural model of rat GGT (green) in comparison with a HuGGT (cyan) model.

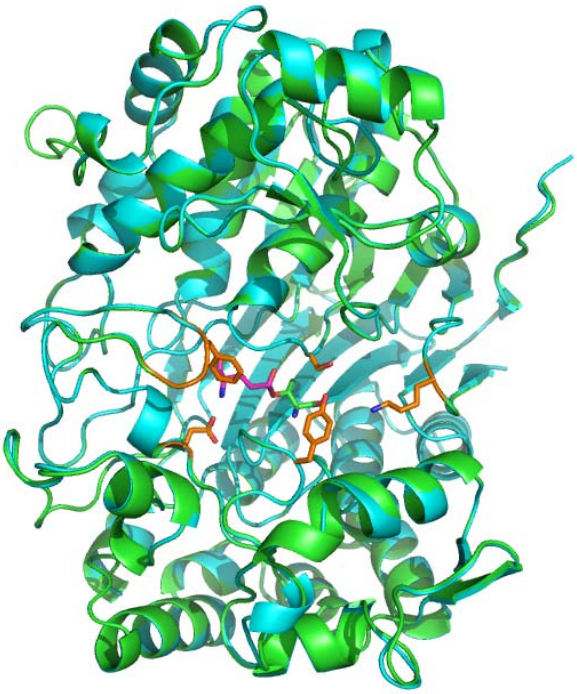

Supplemental Figure S6. Binding interactions of substrate GSH with *E. coli* GGT (EcGGT) and *H. pylori* GGT (HpGGT).

A) **EcGGT/GSH**

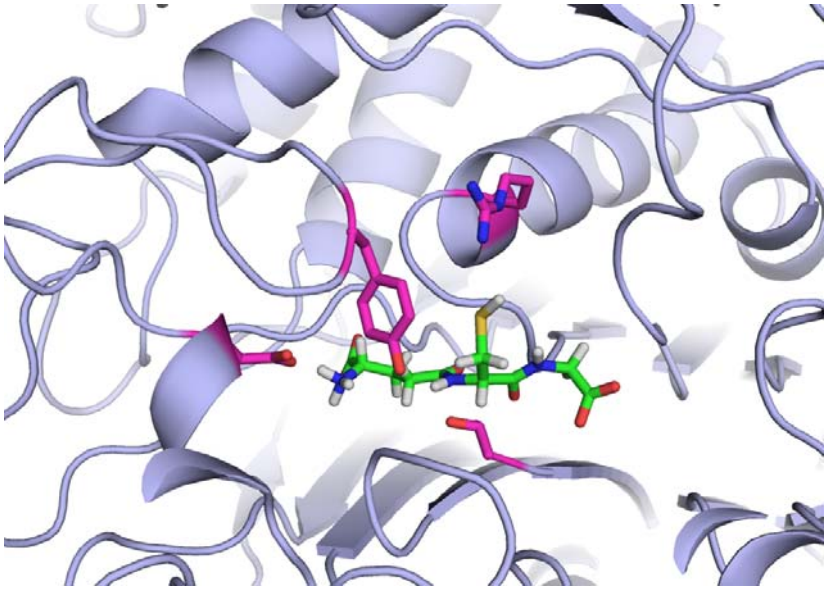

B) **HpGGT/GSH**